DEVELOPMENT OF THE GLOBAL FLUVIAL BIOMASS MODEL CONSIDERING DISTURBANCE

HIKARI MATSUDA
University of Tsukuba, Tsukuba, Japan, s1920936@s.tsukuba.ac.jp

YUI SHINOZAKI
University of Tsukuba, Tsukuba, Japan, yuishinozaki@hotmail.com

NAOKI SHIRAKAWA
University of Tsukuba, Tsukuba, Japan, naoki-s@kz.tsukuba.ac.jp

ABSTRACT

This study is one of the first attempts to assess global environmental flow requirements (EFR), taking into account the effect of disturbance. Shinozaki et al. (2018) proposed the global fluvial biomass model to estimate EFR based on the primary productivity and aquatic plant biomass. Though, like other global models, the model output is a monthly basis and does not consider extreme flow events or disturbance. However, disturbance such as floods plays a critical role in maintaining the functions and diversity of river ecosystems. Therefore, we improved the model by considering disturbance as an increase in shear stress that causes loss of plant biomass. In this model, daily river flow and the river gradient determine the timing and frequency of disturbance. According to Biggs (1996), where the river gradient is steeper than 0.5%, five times the preceding 14 days mean flow was set as the disturbance threshold and 2.5 times in other areas, which causes a 100% loss of plant biomass. The total global amount of aquatic plant biomass was estimated to be 1.06×10^8t. For verifying the model results, we compared calculated biomass with observed values in 15 rivers around the world. We confirmed that the results followed the trend of seasonal fluctuations, and 70% of calculated values fell within the range of the observation sites.

Keywords: Environmental flow, disturbance, algae, biomass, global model

1. INTRODUCTION

Environmental flows describe the quantity, timing, and quality of freshwater flows and levels necessary to sustain aquatic ecosystems which, in turn, support human cultures, economies, sustainable livelihoods, and well-being (Arthington et al., 2018). Water resources are now frequently being exchanged across catchments, and they may also be longitudinal disproportionalities in its availability. In order to assess where enough water is available for withdrawals and meeting other human demands, it is necessary to estimate how much water is needed to sustain freshwater ecosystems at a global scale (Pastor et al., 2014). Several global EFR models have been proposed to this end. As a first attempt, Smakhtin et al. (2004) proposed a global EFR as a percentage of mean annual discharge with a combination of high flow and low flow requirements based on simple hydrological statistics. Hanasaki et al. (2008) estimated annual global EFR depending on the climatic classifications. Pastor et al. (2014) proposed monthly EFR for the first time as global assessment using flow statistics such as Q_{90} and Q_{50}. Shinozaki et al. (2018) proposed a global fluvial biomass model using primary productivity (NPP) and longitudinal transportation of plant biomass. The novel point of this model was that the EFR thresholds were set according to the ecological parameters (productivity and vulnerability) which cannot be evaluated by hydrological statistics. However, global EFR methods are still based on simple hydrological methods, forced by a lack of global ecohydrological data to limit themselves to mean annual discharge and some flow variabilities. Therefore, they do not consider the effects of flood disturbance. Flood disturbance plays a crucial role in improving water quality, creating a new habitat for wildlife, longitudinal and lateral transportation of organic matters and nutrients, and reduce exotic species.

The purpose of this study is to improve the global fluvial biomass model to be able to describe one of the effects of flood disturbance; the loss of plant biomass caused by increase of shear stress. According to the daily flow variations, timing and the number of critical disturbances were determined to reset the biomass accumulation within the channel. We compared the results calculated by the conventional model and the improved model to check the effect of disturbance. We then verified the accuracy of the improved model by comparing with observed values of 15 points in different climatic regions of the world.

2. MODEL

2.1 The global fluvial biomass model

This is a model that calculates the amount of aquatic biomass in the river (Shinozaki et al., 2018). This model focuses on Net Primary Productivity (NPP) to assess the regional characteristics of fluvial ecosystems. NPP is the amount of plant biomass available to support the consumer organisms. Gross primary productivity (GPP) is the rate at which primary producers store energy through photosynthesis, a part of which is consumed for respiration and the remainder accumulated as biomass; the rate describing the latter process is referred to as NPP. Biomass are calculated by the equations below;

$$\frac{\partial B}{\partial t} + \frac{\partial BU}{\partial x} = NPP - dB - pB + \beta B \tag{1}$$

$$U = fV \tag{2}$$

where B is aquatic plant biomass [g/m^2] , NPP is net primary production [g/m^2/day], V is flow velocity [m/s], d is the decrease rate by plant death, p is the decrease rate by grazing, β is the rate of inflow from land, f is the rate of biomass that flow down. In this model, d, p, and f are set as 0.1, 0.0, and 1.0 based on Shinozaki et al. (2018). The first term on the right of the equation is the growth of plants by photosynthesis, the second term is decrease of biomass due to respiration, decomposition and mineralization. The third term is decrease due to predation, and the fourth term is inflow of plant biomass from terrestrial area. U is obtained by multiplying V by the coefficient f. f is determined by exfoliation of attached algae and reduction of the flux rate according to topography and waterworks structures. The aquatic plant (autochthonous) biomass produced within a given area includes attached algae, herbal plankton and detritus which are regarded to have potential as food resources for consumer organisms. Riparian plants and terrestrial woody debris, litter falls, as well as particles of aquatic plant biomass from upstream make up allochothonous biomass. Vegetation rate β is set as 3% of river width is set as riverbank. The model concept is shown in Figure. 1. A grid setup is used to model the river channel network and adjacent terrestrial areas. Flow direction is indicated in each grid cell. In each cell, NPP is given. Since NPP of aquatic vegetation is dependent on channel habitat size, channel habitat size is set using river width and length. River width is calculated from mean monthly discharge and riverbed gradient, assuming that the water course has a triangular cross-section. River length is derived by multiplying grid cell length (Δx) and coefficient of meander (α) (Figure. 1 (a)). Primary production is the main source of plant biomass, in addition to a certain amount (βB) supplied from terrestrial vegetation. A portion of biomass enters the cell from upstream and leaves downstream. To simplify the model, we assumed that the amount of biomass flowing out of the cell corresponds to flow velocity (V) and is defined it as the biomass amount passing along the river length in a specific period. In addition to these processes, a portion of biomass disappears through decomposition and mineralization (Figure 1 (b)). Theoretically, these processes occur simultaneously.

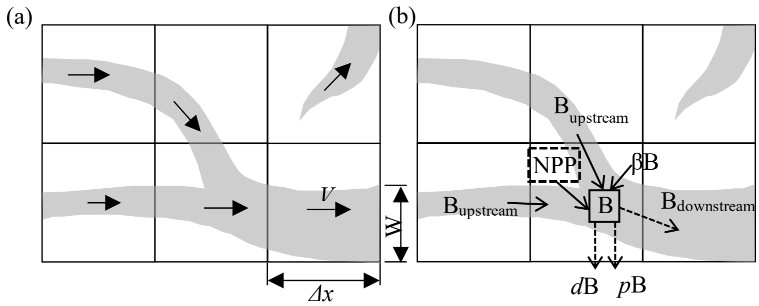

Figure 1. A grid layout used in the model. (a) Grid parameters. Δx: cell length; w: stream width; V: flow velocity. (b) Inputs and outputs of a grid cell. B: biomass, NPP is net primary production, d, p, β, f are coefficients.

3. DISTURBANCE CONSIDERED IN THIS MODEL

Disturbance is a natural event which causes a large change in wildlife habitat. In riverine ecosystem, Increase the flow velocity and shear stress during a flood is considered as one of the major disturbances. Increase the flow velocity and shear stress trigger the exfoliation of attached algae and transportation of plant biomass including algae, CPOM (coarse particle organic matters) and plankton to downstream. Usually, physical removal of attached algae begins when the average velocity exceeds 1m/s (Nakadoi et al., 2012). For example, according to Suetsugi (2002), the flood occurred in Chikuma river in 1998 and 1999 resulted in decrease of plant biomass by 60 percent, after the flood. Aquatic plants and attached algae also be removed from the riverbed and flow down when the shear stress increase. Such disturbance contributes to algae growth promotion and organic matter supply to the downstream.

3.1 Thresholds of disturbance

The disturbance dealt with this paper is flood disturbance which causes the loss of plant biomass by the increase of shear stress. To calculate the shear stress in global scale, we used the river discharge and terrain slope to determine the timing and frequency of disturbance. According to Biggs (1996), where the river gradient typically 0.5%, 5 times the normal flow (preceding 7 day mean flow) causes 0-100% loss of plant biomass. Furthermore, at lower gradient streams, 2.5 times the normal flow can cause some loss of plant biomass (Biggs, 1996). From the above, 5 times the normal flow was set as the disturbance threshold where the river gradient is steeper than 0.5%, and 2.5 times in other areas, which causes a 100% loss of plant biomass. Figure 2 shows the diagram of the new global fluvial biomass model including the effect of disturbance. This model distinguishes two types of biomass; attached biomass and floating biomass. 10% of biomass is set as attached biomass and 90% as planktonic biomass. The flow down rate (*f* in the equation(2))is not applied to attached biomass because it is fixed and grow in the same cell. In addition, every 14 days, 20% of attached biomass is removed and be a part of floating biomass. As long as the discharge exceeds the threshold, the disturbance continues. The maximum duration of a disturbance is ten days which is based on flood experience with the aim of causing artificial disturbance to improve the river environment at Colorado River on March, 1996 (Collier et al., 1997). Figure 3 shows an example of determination of a disturbance. Q' represents the preceding N day mean flow of D_1. When the threshold is n times the normal flow (Q'), since river flow at D_1 exceeds the threshold, it is determined that disturbance occurs in D_1. As the river flow exceeds the threshold during D_1~D_3, disturbance continues until D_3.

In this model, the occurrence of disturbance is determined from daily river flow statistics of ten years. Since disturbance is an uncertain event, it does not happen at the same date every year. In order to identify the approximate timing of disturbance, each month were divided into 3 terms, first (1^{st} - 10^{th}), middle (11^{th} – 20^{th}) and the end (21^{st}- last day). Frequency and duration were calculated for each term. If disturbance occurs more than 5 times in 10 years, it is determined that it occurs at standard year.

3.2 Used data

The model was established based on a global river channel network and catchment data from the 30' global drainage map (DDM30) by Döll et al. (2002), with a spatial resolution of 0.5°×0.5° (360 × 720 grid cells worldwide). River velocity, depth, and width were calculated using the manning's equation and the discharge. The discharge is calculated by the H08 model (Hanasaki et al., 2008). Average annual daily river flow of 2001-2010 was used for simulation. River flow is calculated from the WFDEI meteorological forcing data set (Weedon et al., 2011). The average monthly terrestrial NPP from 2001 to 2010 was used as aquatic NPP. NPP and vegetation cover data are obtained from NASA Earth Observatory. Aquatic NPP is usually affected by nutrient concentration and turbidity, though since solar radiation is the controlling factor of both land and aquatic NPP, the terrestrial NPP was used as aquatic NPP. The Harmonized World Soil Database v1.2 by the Food Agriculture Organization (2012) was used as global slope data.

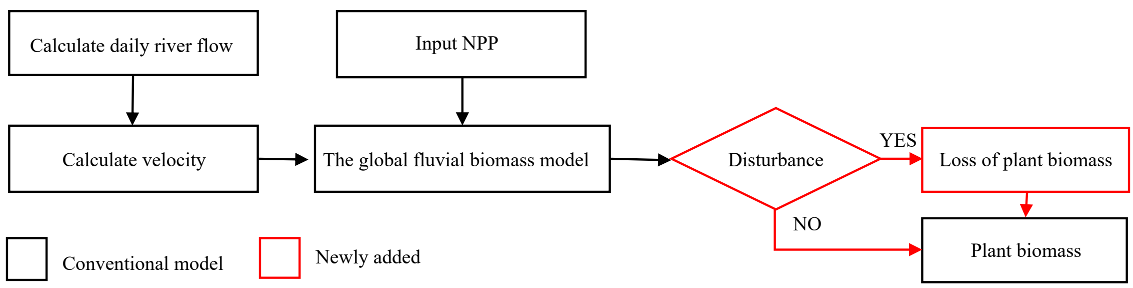

Figure 2. Image of setting disturbance

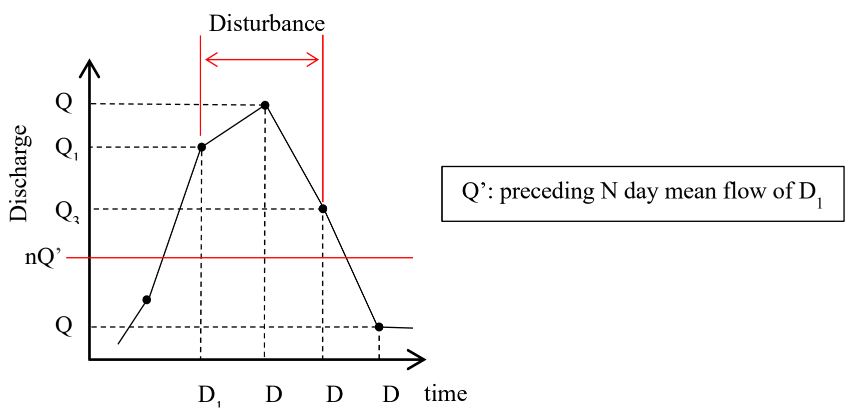

Figure 3. Disturbance Setting in this Model

4. VERIFICATION OF THE DISTURBANCE THRESHOLDS

Although Biggs determined normal flow as preceding 7-day mean flow, in this model, preceding 14-day mean flow was used as the normal flow. Because the model resolution is 0.5 degrees, multiple river channels in a grid are combined into one channel to calculate discharge. For this reason, the representative hydrograph is gentler than the individual hydrographs of each river in the grid. Thus, it is hard to capture a sharp increase in the calculation. Therefore, a 7-day mean flow cannot capture the disturbance at a global scale. Instead of this, we used the preceding 14-day mean flow, after the following validation with an actual river, which is the growth cycle of algal.

The occurrence of disturbance was verified using calculated and observed river flow. As observed data, the daily river flow of 2010 at Fuji River in Japan was used (MLIT, 2010). Figure 4 shows the observed daily discharge of Kitamatsuno Station at Fuji River and the threshold of disturbance, which is 2.5 times the preceding 7-day mean flow (hereinafter, "threshold A"). Figure 5 shows the calculated daily river flow and threshold. In addition to threshold A, 2.5 times the preceding 14-day mean flow (hereinafter, "threshold B") is shown in the Figure. The peak flow calculated by H08 tends to be overestimated, however, it captures the general trends of seasonal flow variabilities. Table 1 shows the number of disturbances determined by calculation and observation flow. As a result, the estimate using the threshold B is closer to the observed outcome. Therefore, normal flow is defined as preceding 14 days mean flow in this model.

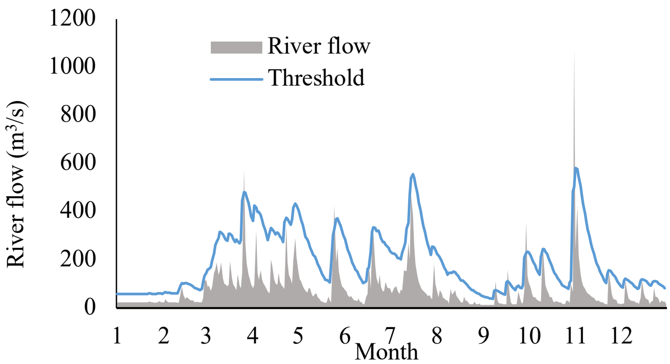

Figure 4. Observed daily river flow of Fuji River and threshold of disturbance.
The threshold is 2.5 times the preceding 7-day mean flow (Threshold A).

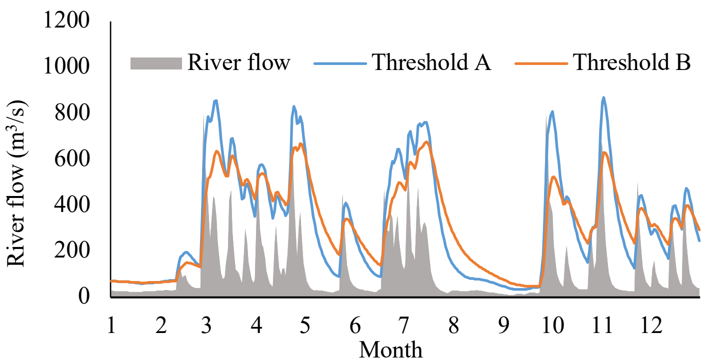

Figure 5. Calculated daily river flow of Fuji River and threshold of disturbance.
Threshold A is 2.5 times the preceding 7 day mean flow. B is 2.5 times the preceding 14-day mean flow.

Table 1. Number of disturbances

	Observation	**Calculation**	
		Threshold	
	A	A	B
Jan	0	0	0
Feb	2	2	2
Mar	1	0	0
Apr	1	2	2
May	1	1	1
Jun	2	1	2
Jul	1	0	1
Aug	0	0	0
Sep	3	1	1
Oct	3	2	2
Nov	1	1	1
Dec	2	2	2
Sum	17	12	14

5. RESULTS

5.1 Number of Disturbances

The calculated disturbance in this model is shown in Figure 6. It represents for the number of times of disturbance that occurred during a year. The most frequent disturbance occurs in Ecuador (1° 25"S, 77°25"W) and is 25 times a year. Disturbance tends to occur frequently at low latitude area especially tropical savanna climate zone. At South Asia such as India and Nepal, disturbance occurs in summer which is the main monsoon season. At countries in Southeast Asia, disturbance occurs frequently in the wet seasons, roughly June to November. European countries such as England and Ireland are also disturbance-prone area, which occurs in relatively wet season in winter.

5.2 Global fluvial biomass

5.2.1 Result of calculation

Using the disturbance calculated above, global biomass was estimated. Figure 7 shows the distribution of annual average biomass. The global annual average amount of biomass was 1.06×10^8 t. The calculated result without considering disturbance was 1.07×10^8 t. This falls within the range of estimates from the previous studies which is 0.40×10^8 t~1.45×10^9t (Shinozaki et al., 2018). The global average amount of biomass decreased by 0.93% if considering disturbance. Though we attempted to describe the effect of disturbance in the model, there was small difference in the global total.

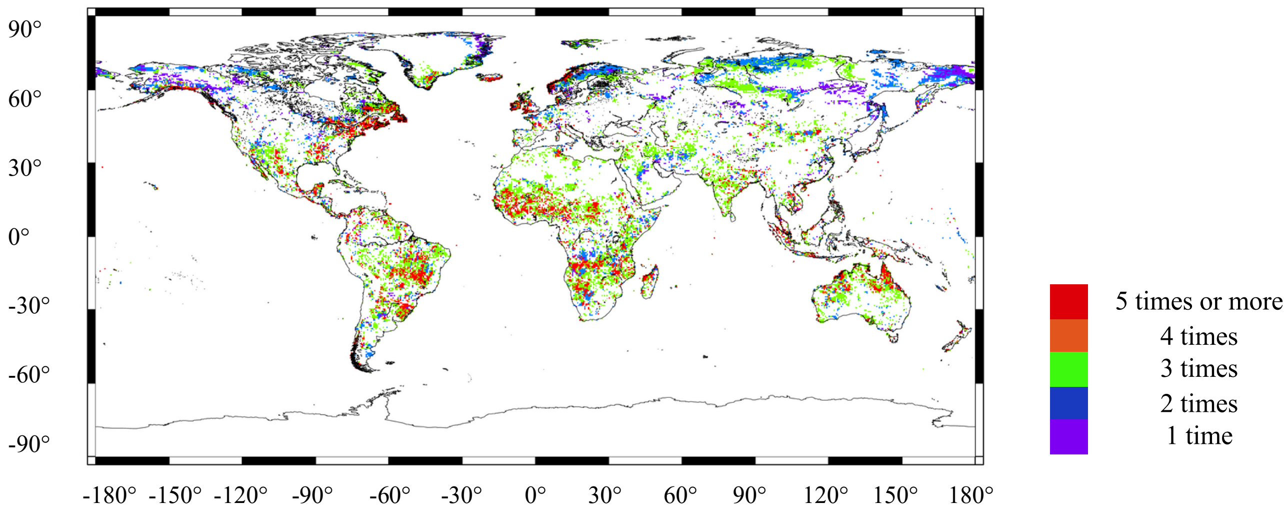

Figure 6. Number of occurrences of disturbance

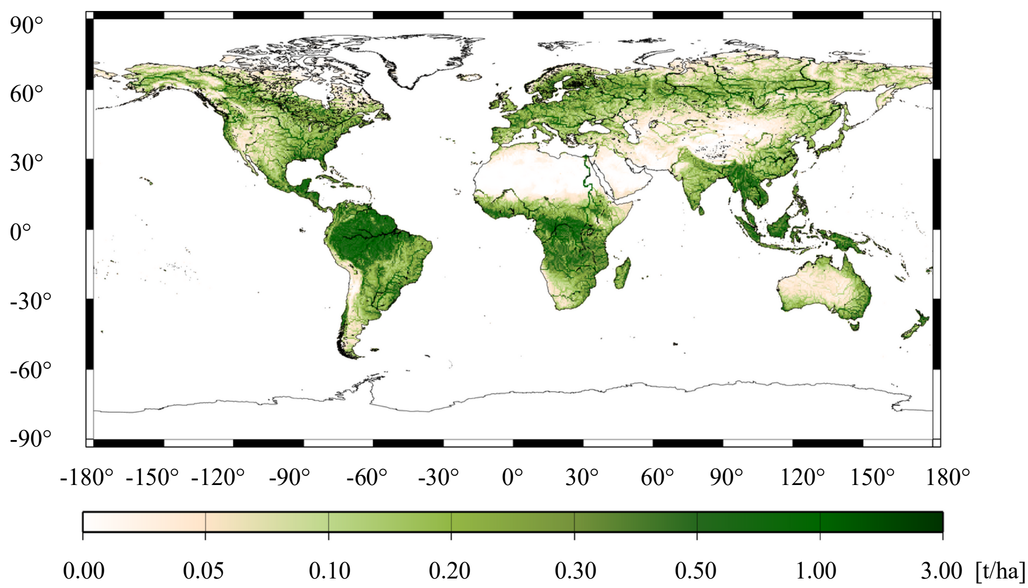

Figure 7. Annual average amount of biomass

However, at the regional scale, the results of the biomass differed depending on whether or not disturbance was considered. Figure 8 displays the reduction rate of annual average calculated biomass after considering disturbance. In areas belong to tropical savanna climate zone such as Northern Australia, Mid Africa, and places where are affected by monsoon and cyclones such as Indonesia and Madagascar, biomass decreased by more than 5%. Comparing Figure 8 and Figure 6, despite that disturbance occurred in high latitude area such as Greenland and northern Russia, there is no difference in biomass, because the NPP itself is small in such regions.

5.2.2Verification

To confirm how the disturbance affects the amount of biomass in this model, the annual biomass fluctuation is illustrated. Figure 9 shows the annual change of biomass of Mogami River. From the graph it is confirmed that the new model succeeded in demonstrating the effect of disturbance. The disturbance occurs in February, June and September. Each disturbance represents snowmelt, heavy rains during rainy season, and floods by typhoon respectively. The graph shows that all plant biomass is washed away at the time of disturbance. Though plant biomass become zero immediately after the disturbance, it quickly recovers the same level of the case without considering the disturbance. On average, biomass takes 22 days to be to same value of the conventional model.

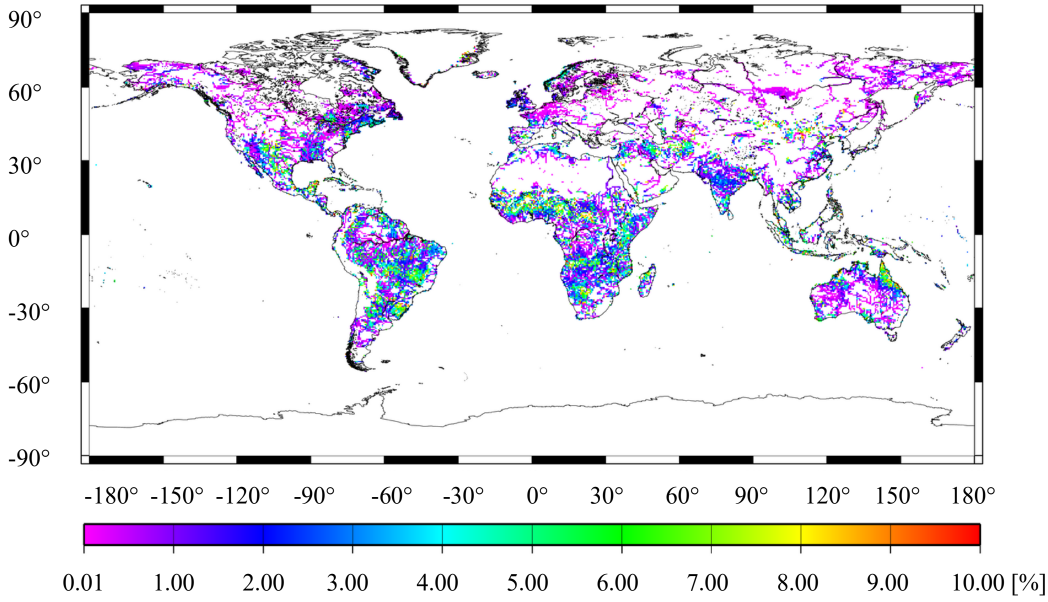

Figure 8. Biomass reduction rate of each cell

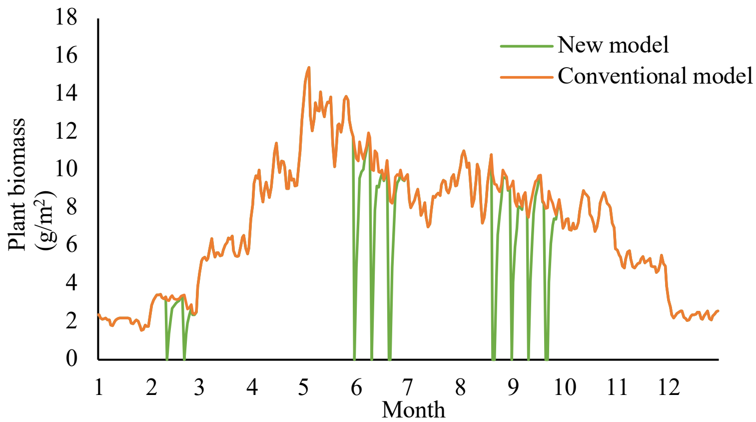

Figure 9. Annual change of biomass

6. DISCUSSIONS

Calculated results were compared with the observed value of 15 rivers of the world (Figure 10). References are shown in Table 2. The amount of plant biomass in a river varies greatly depending on the flow condition, season, and measurement method even at the same point. The difference may become 10^2 times, as can be seen from the observation range in Figure. 10. The reason is that aquatic plants are easily washed away by flooding, that the generation shift is fast (weeks or months), and that the biomass changes significantly due to slight environmental changes. Even without disturbance, biomass in successive years can vary by as much as twice (Mulholland, 1981). As it can be seen from the fluctuation range of Yangtze River, plant biomass has a hundred-time difference even if it is the same point. Therefore, if the calculated value fit in this range it indicates the model value is acceptable. From Figure 10, biomass calculated by the new model of 11 points fits in this range. On the whole, it tends to be overestimated compared to the observed value, especially in small streams such as

Bear Brook, White Clay Creek, and Logan River. H08 overestimates the results in small basins because the calculated flow equals to the total flow of all river channels in the grid. This is the performance limit of the global model.

Table 3 shows the rate of reduction by disturbance of annual average amount of plant biomass for each observation point. The reduction rate of Ilha Grande and Bear Brook are 2.99% and 5.28% respectively, which are greater than the global average rate (0.93%). Since the simulation resolution is 0.5°×0.5°, these small streams are represented in one grid cell. Therefore, inflow from upstream are not calculated and only decrement by disturbance is reflected in calculation.

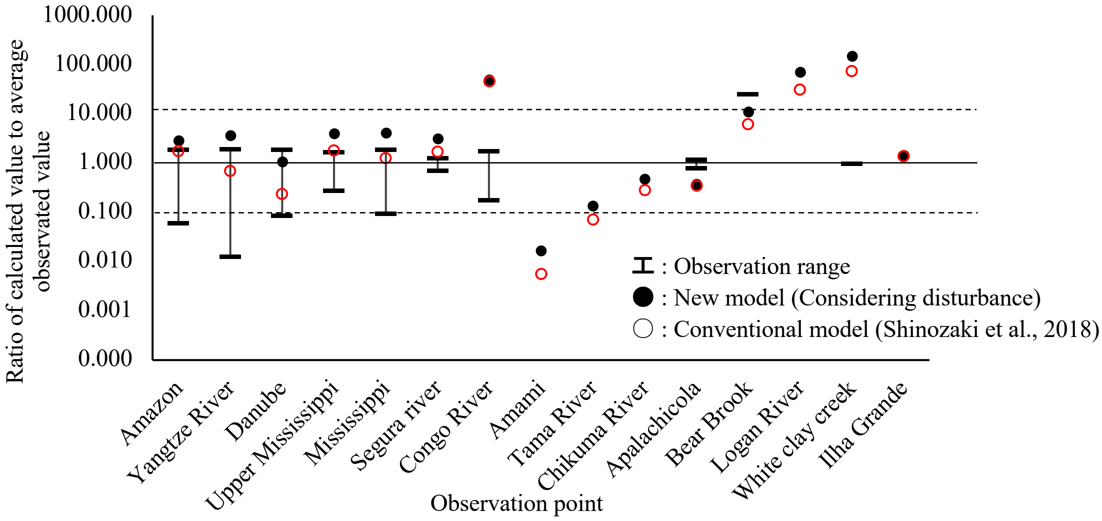

Figure 10. Ratio of calculated value of annual average biomass to observed value.

Table 2. References of the observation value

Observation point		Reference
Amazon	Brazil	Costa (2005)
Yangtze River	China	Humborg (1997)
Danube	Germany	
Mississippi	U.S.A.	
Congo River	Congo	
Upper Mississippi	U.S.A.	Webster et al. (1997)
Segura River	Spain	Velasco et al. (2003)
Amami	Japan	Abe et al. (2008)
Tama River	Japan	Aizaki (1980)
Chikuma River	Japan	Yagi (1983)
Apalachicola	Canada	Behzad et al. (2000)
Bear Brook	U.S.A.	Pennak et al. (1979)
White clay creek	U.S.A.	
Ilha grande	Brazil	Moulton et al. (2015)

Table 3. Comparison of calculated results and reduction rate

Basin	Observation point	Calculated Value (t/ha/y) ①With disturbance	②Without disturbance	Reduction rate①/② (%)
Estuary	Yangtze	26.49	26.60	0.39
	Danube	22.44	22.46	0.08
	Ilha Grande	0.59	0.61	2.99
	Mississippi	20.07	20.13	0.28
	Congo	25.36	25.44	0.28
	Apalachicola	2.84	2.84	0.00
Downstream	White clay creek	2.54	2.54	0.00
	Amazon	27.65	27.71	0.22
	Segura	3.16	3.17	0.46
Middlestream	Tama	2.02	2.02	0.00
	Chikuma	2.87	2.87	0.00
	Upper Mississippi	2.81	2.81	0.00
	Bear Brook	5.13	5.41	5.28
Upper stream	Logan	1.80	1.80	0.00

7. CONCLUSIONS

The conventional global fluvial biomass model was improved and become able to consider the effect of increase in shear stress. Our model represents for flood disturbance mainly occurs in low latitude areas and calculate amount of aquatic plant biomass considering disturbances. Globally, annual average amount of biomass decreased by only 0.93% due to disturbance. In regional scale, more than 5% of biomass decreased at areas near the equator, while there were almost no changes at high latitude area despite of disturbance. In this paper, we also compared the calculated results with the observed value of 15 rivers. Overall the calculation value are slightly above the observation value, and 70% fall within the observation range. We still have following challenge to overcome: to describe the other effect of disturbance which is the inflow from the floodplain.

REFERENCES

Abe, S., Iguchi, K., Yonezawa, T., and Shinomiya, A. (2008). Flora and primary productivity of stream periphyton in habitats of Plecoglossus altivelis ryukyuensis in Amami-Oshima Island, Japan. *The bulletin of Japanese Society of Phycology*, 56(1):9-16.

Aizaki, M. (1980). Changes in Standing Crop and Photosynthetic Rate attendant on the Film Development of Periphyton in a Shallow Eutrophic River. *Jap. J. Limnol.*, 41(4):225-234.

Arthington, Angela H, et al. (2018). The Brisbane Declaration and Global Action Agenda on Environmental Flows (2018). *Frontiers in Environmental Science 6*, 45: 1-15.

Behzad Mortazav, Richard L. Iverson, William M. Landing, F. Graham Lewis and Wenrui Huang. (2000). Control of phytoplankton production and biomass in a river-dominated estuary: Apalachicola Bay, Florida, USA. *Marine Ecology Progress Series,* 198:19-31.

Biggs, B.J.F. (1996). Hydraulic habitat of plants in streams, Regulated rivers. *research management,* 12:131-144.

Collier, M.P., Webb, R.H., Andrews, E.D. (1997). Experimental flooding in Grand Canyon. *Scientific American*, 276(1):82-89.

Costa, M. (2005). Estimate of net primary productivity of aquatic vegetation of the Amazon floodplain using Radarsat and JERS ‐ 1. *International Journal of Remote Sensing*, 26(20): 4527-4536.

Döll, P., Kaspar, F. and Lehner, B. (2002). Validation of a new global 30-min drainage direction map. *J. Hydrol.*, 258:214-231.

FAO, IIASA, ISRIC, ISS-CAS, and JRC. (2012). Harmonized World Soil Database (version 1.2). FAO, Rome, Italy and IIASA, Laxenburg, Austria.

Hanasaki, N., Kanae, S., Oki, T., Masuda, K., Motoya, K., Shirakawa, N., Shen, Y., and Tanaka, K. (2008). An integrated model for the assessment of global water resources - Part1: Model description and input meteorological forcing. *Hydrol. Earth Syst. Sc.*, 12:1007-1025.

Humborg, C. (1997). Primary Productivity Regime and Nutrient Removal in the Danube Estuary, Estuarine. *Coastal and Shelf Science*, 45: 579-589.

Ministry of Land, Infrastructure, Transport and Tourism. (2010). Water Information System. *http://www1.river.go.jp*

Moulton, T.P., Lourenço-Amorim, C., Sasada- Sato, C.Y., Neres-Lima, V., Zandonà, E. (2015). Dynamics of algal production and ephemeropteran grazing of periphyton in a tropical stream. *International review of Hydrobiology*, 100:61-68.

Mulholland, P J. (1981). Organic carbon flow in a swamp-stream ecosystem. *Ecol. Monogr.,* 51:307–322.

Nakadoi, Y., Tsubaki, R., and Kawahara, Y. (2012). Refinement of evalutation model for attached-algae removal considering removal patterns. *Journal of Japan Society of Civil Engineers. Ser. B1*, *Hydraulic engineering*, 68(4): I_751-I_756.

Pastor,A.V., Ludwig F.L., Biemans, H., Hoff, H. and P, Kabat. (2014). Accounting for environmental flow requirements in global water assessments. *Hydrol. Earth Syst. Sc.*, 18:5041-5059.

Pennak, R.W., and James, W. Lavelle. (1979). In situ measurements of net primary production in a colorado mountain stream. *Hydrobiologia*, 66(3):227-235.

Shinozaki, Y., Shirakawa, N., and Fujiwara, M. (2018). Global environmental flow requirement based on primary productivity and vulnerability of fluvial ecosystems. *12th International Symposium of Ecohydraulics*, *Tokyo.*

Shinozaki, Y., Fujiwara, M., Shirakawa, N. (2018). Global monthly environmental flow requirement based on the net primary productivity of rivers. *Journal of Japan Society of Civil Engineers, Ser. G (Environmental Research)*, 46: II-85

Smakhtin, V, Revenga, C. and Döll, P. (2004). A pilot Global Assessment of Environmental Water Requirements and Scarcity. *Water International*, 29(3):307-317.

Suetsugi, T. (2002). The relationship between disturbance of ecological system and the characteristics of geomorphology and floods. *Japanese Journal of Ecology*, 52:275-279.

Velasco, J., Millan, A., Vidal-Abarca M.R., Suarez, M.L., Guerrero, C. and Ortega, M. (2003). Macrophytic, epipelic and epilithic primary production in a semiarid Mediterranean stream. *Freshwater Biology*, 48:1408-1420.

Webster, J.R. and Meyer, J.L. (1997). Stream Organic Matter Budgets: An Introduction. *Journal of the North American Benthological Society*, 16(1):3-13

Weedon G.P., Gomes S., Viterbo, P., Shuttleworth, W. J., Blyth, E., Österle, H., Adam, J.C., Bellouin, N., Boucher, O., and Best, M. (2011). Creation of the WATCH forcing data and Its use to assess global and regional reference crop evaporation over land during the twentieth century. *Journal of Hydrometeorology*, 12:823-848.

Yagi, A. (1983), Photosynthetic Rate of Sessile Algae in the Lower Kiso River. *Journal of the Nagoya Women's College*, 29:79-83